



**HAL**  
open science

## Probing the local structure of Prussian blue electrodes by $^{113}\text{Cd}$ NMR spectroscopy

A. Flambard, A Sugahara, S De, M Okubo, A Yamada, Rodrigue Lescouëzec

► **To cite this version:**

A. Flambard, A Sugahara, S De, M Okubo, A Yamada, et al.. Probing the local structure of Prussian blue electrodes by  $^{113}\text{Cd}$  NMR spectroscopy . Dalton Transactions, 2017, 46 (19), pp.6159-6162. 10.1039/C7DT00728K . hal-01558174

**HAL Id: hal-01558174**

**<https://hal.sorbonne-universite.fr/hal-01558174>**

Submitted on 10 Jul 2017

**HAL** is a multi-disciplinary open access archive for the deposit and dissemination of scientific research documents, whether they are published or not. The documents may come from teaching and research institutions in France or abroad, or from public or private research centers.

L'archive ouverte pluridisciplinaire **HAL**, est destinée au dépôt et à la diffusion de documents scientifiques de niveau recherche, publiés ou non, émanant des établissements d'enseignement et de recherche français ou étrangers, des laboratoires publics ou privés.

## Probing Local Structure of Prussian Blue Electrodes by $^{113}\text{Cd}$ NMR Spectroscopy

A. Flambard,<sup>a</sup> A. Sugahara,<sup>b</sup> S. De,<sup>a</sup> M. Okubo,<sup>b</sup> A. Yamada<sup>b</sup> and R. Lescouëzec<sup>a</sup>

DOI: 10.1039/x0xx00000x

www.rsc.org/

**We demonstrate that  $^{113}\text{Cd}$  NMR is a potent technique to monitor the local electronic and structural states of the Prussian blue electrode during  $\text{Li}^+$  intercalation, providing an atomic-scale insight into the reaction mechanism.**

Prussian blue, also called ferrous ferrocyanide, is the oldest synthetic coordination polymers.<sup>1</sup> Originally used as pigment in the 18<sup>th</sup> and 19<sup>th</sup> centuries, it has known a rebirth in the last decades through the study of its analogues of general formula  $\text{A}_n\text{M}'_x[\text{M}(\text{CN})_6]_y(\text{H}_2\text{O})_z$  (A : alkali cation; M and M' : transition metal ions). The versatile (nanoporous) structure and tuneable electronic properties of the Prussian blue analogues (PBAs) offer many potential applications in material science. PBAs have been explored for (hydrogen) gas storage,<sup>2</sup> (bio)sensing,<sup>3</sup> heterogeneous catalysis,<sup>4</sup> or as molecular magnetic materials.<sup>5</sup> More recently, application of PBAs to the battery electrodes have attracted considerable interests, because of their excellent intercalation properties of various cations ( $\text{Li}^+$ ,  $\text{Na}^+$ ,  $\text{K}^+$ ,  $\text{Mg}^{2+}$ ,  $\text{Ca}^{2+}$ ,  $\text{Al}^{3+}$ , etc.) in both aqueous and non-aqueous electrolytes.<sup>6–15</sup> For example,  $\text{Na}_2\text{Fe}[\text{Fe}(\text{CN})_6] \cdot 0.1\text{H}_2\text{O}$  as a positive electrode material for non-aqueous Na-ion batteries exhibits a large specific capacity of 155 mAh/g at the average potential of 3.1 V vs.  $\text{Na}/\text{Na}^+$ .<sup>16</sup> However, the reaction mechanism of the PBA electrodes have not been fully understood yet. Gaining information on the structural and electronic changes occurring in the host material at the atomic scale is now crucial to improve the batteries performance.<sup>17–21</sup> For cathodes materials containing iron ions,  $^{57}\text{Fe}$  Mössbauer spectroscopy allows to probe the redox state of the active iron(II/III) ions.<sup>22</sup> In the field of Li-ion batteries,  $^6\text{Li}/^7\text{Li}$  NMR is also often used to investigate the  $\text{Li}^+$  (de)intercalation processes during the charge and discharge.<sup>23–25</sup> Indeed  $^6\text{Li}/^7\text{Li}$

NMR allows to probe the chemical environment surrounding  $\text{Li}^+$  ions, providing information concerning the host material at the local scale. However,  $^7\text{Li}$  NMR signal is broadened by homonuclear dipolar coupling and the second-order quadrupolar interaction while the receptivity of  $^6\text{Li}$  nuclei ( $I = 1$ ) is relatively small (3.58 vs.  $^{13}\text{C}$ ). In contrast, in this work, we chose to directly investigate the local changes occurring in the electrode material by measuring an NMR active nuclei belonging to the host framework. We selected the  $\text{Cd}^{\text{II}}[\text{Fe}^{\text{III}}(\text{CN})_6]_{2/3} \cdot \square_{1/3} \cdot n\text{H}_2\text{O}$  nanoporous material as a model for investigating  $\text{Li}^+$  (de)intercalation in PBA materials. Actually, the receptivity of  $^{113}\text{Cd}$  ( $I = 1/2$ , 7.67 vs.  $^{13}\text{C}$ ) is higher than that of  $^6\text{Li}$ . Moreover, some of us have previously demonstrated that  $^{113}\text{Cd}$  nuclei is highly sensitive to the redox states of its neighbouring ions in PBA frameworks.<sup>26,27</sup> In fact by studying the two families of PBAs,  $\text{CsCd}^{\text{II}}[\text{M}^{\text{III}}(\text{CN})_6]$  and  $\text{Cd}^{\text{II}}[\text{M}^{\text{III}}(\text{CN})_6]_{2/3} \cdot \square_{1/3} \cdot n\text{H}_2\text{O}$  ( $\square$ :  $[\text{M}^{\text{III}}(\text{CN})_6]$  vacancy; M = diamagnetic  $\text{Co}^{\text{III}}$  or paramagnetic  $\text{Fe}^{\text{III}}$ ) by  $^{113}\text{Cd}$  MAS NMR spectroscopy we showed that  $^{113}\text{Cd}$  NMR can provide accurate information on the local structure of these materials. More specifically, whereas other techniques such as Mössbauer spectroscopy barely reveal the possible existence of different  $\{\text{M}(\text{NC})_x(\text{OH})_{6-x}\}$  sites in PBA frameworks,<sup>28</sup>  $^{113}\text{Cd}$  NMR allowed an accurate identification and quantification of these different sites.<sup>26,27</sup> Therefore, we performed here  $^{113}\text{Cd}$  MAS NMR spectroscopy at different stages of  $\text{Li}^+$  intercalation to characterize the electrochemical reaction in the  $\text{Cd}^{\text{II}}[\text{Fe}^{\text{III}}(\text{CN})_6]_{2/3} \cdot \square_{1/3} \cdot n\text{H}_2\text{O}$  PBA.

The CdFe PBA,  $\text{Cd}^{\text{II}}[\text{Fe}^{\text{III}}(\text{CN})_6]_{2/3} \cdot 4.7\text{H}_2\text{O}$ , was synthesized by a precipitation method.<sup>26</sup> The X-ray diffraction (XRD) pattern (Figure S1) for the precipitated compound yields a unit cell parameter of 10.83 Å ( $Fm\bar{3}m$ ). The electrochemical  $\text{Li}^+$  (de)intercalation in 1M  $\text{LiClO}_4$ /propylene carbonate (PC) was conducted using a galvanostatic intermittent titration technique<sup>29</sup> as shown in Figure 1. The resulting potential profile and the open circuit potentials indicate that reversible 0.5 $\text{Li}^+$  (de)intercalation occurs per the formula unit (i.e.,  $\text{Li}_x\text{Cd}[\text{Fe}(\text{CN})_6]_{2/3} \cdot 4.7\text{H}_2\text{O}$ ,  $0 < x < 0.5$ ) approximately between 3.7 and 3.3 V vs.  $\text{Li}/\text{Li}^+$ , associated with the reversible redox

<sup>a</sup> Sorbonne Universités, UPMC Paris 6, Institut Parisien de Chimie Moléculaire, CNRS UMR 8232, 4 place Jussieu, Paris 75252, France

<sup>b</sup> Department of Chemical System Engineering, School of Engineering, The University of Tokyo, Hongo 7-3-1, Bunkyo-ku, Tokyo 113-8656, Japan

Electronic Supplementary Information (ESI) available: [details of any supplementary information available should be included here]. See DOI: 10.1039/x0xx00000x

reaction of the  $[\text{Fe}^{\text{III}}(\text{CN})_6]^{3-}/[\text{Fe}^{\text{II}}(\text{CN})_6]^{4-}$  couple in the PBA framework. The *ex situ* XRD experiment confirms that the  $\text{Li}^+$  (de)intercalation proceeds through a solid solution reaction (Figure S2-S3). All the electrochemical properties of the CdFe PBA electrode are similar to those reported for the other hexacyanoferrate-based PBA electrodes.<sup>22,30</sup>

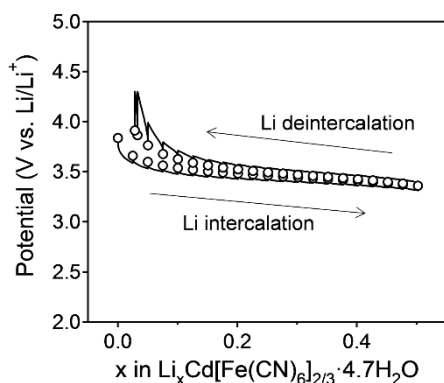


Fig. 1 Open circuit voltages (open circles) of the  $\text{Cd}[\text{Fe}(\text{CN})_6]_{2/3} \cdot 4.7\text{H}_2\text{O}$  electrode upon electrochemical  $\text{Li}^+$  ion (de)intercalation in 1 M  $\text{LiClO}_4/\text{PC}$ . The solid line denotes potential profile during the galvanostatic intermittent titration.

In order to probe the changes in the structural and electronic states upon (de)lithiation, the  $^{113}\text{Cd}$  MAS NMR spectra were recorded for the CdFe PBA electrodes at different states-of-charge (Figure 2). The spectrum of the pristine compound,  $\text{Cd}[\text{Fe}(\text{CN})_6]_{2/3} \cdot 4.7\text{H}_2\text{O}$  (**1**), exhibits three different cadmium sites, which were observed and identified in previous studies.<sup>26,27</sup> The isotropic chemical shift values observed at  $-995$ ,  $-1300$ , and  $-1500$  ppm are respectively ascribed to  $\{\text{Cd}(\text{NC}-\text{Fe}^{\text{III}})_3(\text{OH}_2)_3\}$ ,  $\{\text{Cd}(\text{NC}-\text{Fe}^{\text{III}})_4(\text{OH}_2)_2\}$  and  $\{\text{Cd}(\text{NC}-\text{Fe}^{\text{III}})_5(\text{OH}_2)\}$  sites. In fact, the more  $\text{Fe}(\text{III})$  paramagnetic ions are connected to the Cd ion, the more spin density is delocalized on the Cd ion, leading to a more negative chemical shift. The signal arising from the  $\{\text{Cd}(\text{NC}-\text{Fe}^{\text{III}})_4(\text{OH}_2)_2\}$  site slightly splits due to the cis/trans isomer surroundings.<sup>26</sup>

Ideally, for each intercalated  $\text{Li}^+$  ion, one  $\text{Fe}(\text{III})$  ion should be reduced to a  $\text{Fe}(\text{II})$  one. Hence, one can expect the appearance of signals at lower chemical shift upon  $\text{Li}^+$  intercalation, which are ascribed to new Cd sites where one or several surrounding iron ions are reduced. The general formula for these sites is  $\{\text{Cd}(\text{NC}-\text{Fe}^{\text{III}})_n(\text{dia})_{6-n}\}$ , where "dia" refers to either  $\text{H}_2\text{O}$  or  $(\text{NC}-\text{Fe}^{\text{II}})$  moieties. Indeed, the experimental spectra show that, upon  $\text{Li}^+$  intercalation from  $x = 0$  (**1**) to 0.18 (**2**), the relative intensity of the signals corresponding to the  $\{\text{Cd}(\text{NC}-\text{Fe}^{\text{III}})_4(\text{dia})_2\}$  and  $\{\text{Cd}(\text{NC}-\text{Fe}^{\text{III}})_5(\text{dia})\}$  sites decrease whereas an increase of intensity and a broadening are observed for the  $\{\text{Cd}(\text{NC}-\text{Fe}^{\text{III}})_3(\text{dia})_3\}$  site (originally near  $-995$  ppm). This broadening may be related to the existence of different sites such as  $\{\text{Cd}(\text{NC}-\text{Fe}^{\text{III}})_3(\text{NC}-\text{Fe}^{\text{II}})_2(\text{OH}_2)_2\}$  or  $\{\text{Cd}(\text{NC}-\text{Fe}^{\text{III}})_3(\text{NC}-\text{Fe}^{\text{II}})(\text{OH}_2)_2\}$ , which are expected to exhibit similar chemical shifts, because the paramagnetic chemical shift is

dominant over the diamagnetic one as mentioned in our previous study.<sup>26</sup> Another interesting observation is the occurrence of a new peak located at  $-440$  ppm, which accounts for a new cadmium site having more diamagnetic neighbours. The chemical shift anisotropy of this signal is particularly large in comparison to the other signals. Indeed complementary experiments carried out at different spinning speeds confirm that the two small peaks on both sides are due to spinning side bands (Figure S4). The changes observed in sample (**3**) with  $x = 0.38$  confirms these trends: (i) the signals corresponding to the initial cadmium sites (sites with three, four and five  $\text{Fe}(\text{III})$  neighbouring centres) completely disappeared; (ii) the relative intensity of the signal located at  $-440$  ppm increases significantly; (iii) a small new signal is observed at  $+92$  ppm, which corresponds to a cadmium ion linked only to diamagnetic species. Overall, all these changes are coherent with a reduction of some  $\text{Fe}(\text{III})$  ions to  $\text{Fe}(\text{II})$  ions upon  $\text{Li}^+$  intercalation.

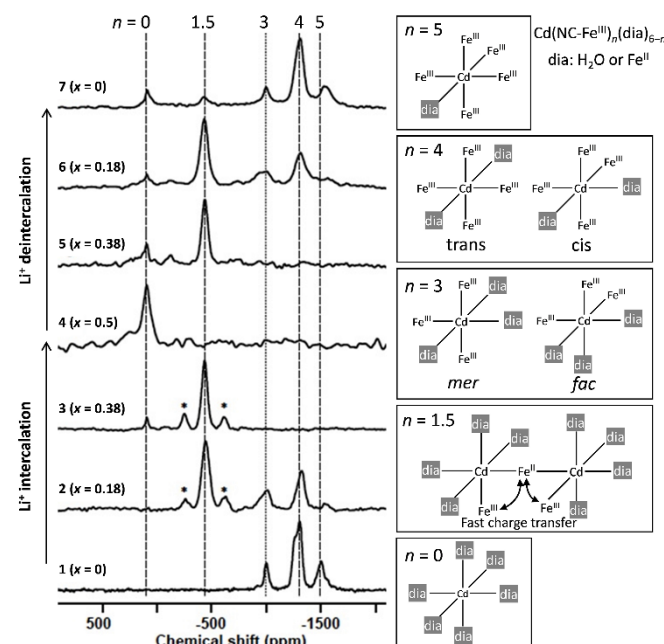


Fig. 2  $^{113}\text{Cd}$  MAS NMR spectra (7.1 T) of  $\text{Li}_x\text{Cd}[\text{Fe}(\text{CN})_6]_{2/3} \cdot 4.7\text{H}_2\text{O}$  recorded at 20 kHz and 272 K. Dotted lines refer to different cadmium environments with different numbers of neighbouring  $\text{Fe}^{\text{III}}$  paramagnetic ions. (\*) spinning sidebands. The Cd sites  $\text{Cd}(\text{NC}-\text{Fe}^{\text{III}})_n(\text{dia})_{6-n}$  are illustrated schematically.

However, it should be emphasized that only one new intense paramagnetic signal around  $-440$  ppm is observed instead of the two expected ones: one for  $\{\text{Cd}(\text{NC}-\text{Fe}^{\text{III}})_2(\text{dia})_4\}$  and one for  $\{\text{Cd}(\text{NC}-\text{Fe}^{\text{III}})_1(\text{dia})_5\}$ . The observed chemical shift is intermediate between those reported for the  $\{\text{Cd}^{\text{II}}(\text{NC}-\text{Fe}^{\text{III}})_2(\text{dia})_4\}$  and  $\{\text{Cd}^{\text{II}}(\text{NC}-\text{Fe}^{\text{III}})(\text{dia})_5\}$  sites in the model compounds.<sup>26</sup> Moreover, this peak cannot be ascribed to a cadmium site linked with two  $\text{Fe}(\text{III})$  centres, because there is no signal at a lower chemical shift (between at  $-440$  and  $+92$  ppm) for the  $\{\text{Cd}^{\text{II}}(\text{NC}-\text{Fe}^{\text{III}})_1(\text{dia})_5\}$  site. The value of the

chemical shift better matches with an average presence of 1.5 Fe(III) per Cd. Interestingly this result points to the occurrence of a fast charge transfer (as compared to the  $^{113}\text{Cd}$  NMR time scale at 7.1 T) between the Fe(III) and Fe(II) ions in the mixed valence materials containing significant amounts of inserted  $\text{Li}^+$  ions. It is worth noticing that the Mössbauer spectrum of **3** shows distinguishable  $\text{Fe}^{3+}/\text{Fe}^{2+}$  contributions, indicating that the charge transfer is slower than  $10^{-7}$  s (Figure S5). The higher local anisotropy observed for this site may be due to the presence of the inserted  $\text{Li}^+$  ions. The alkali ions are expected to interact with the cyanide bridges<sup>31</sup> thus lowering the local symmetry of the Cd sites. Moreover, the anisotropy of the “averaged” cadmium sites ( $\{\text{Cd}^{\text{II}}(\text{NC-Fe}^{\text{III}})_{1.5}(\text{dia})_{4.5}\}$ ) may reflect the different local surroundings of the individual sites.

Upon further  $\text{Li}^+$  intercalation, all paramagnetic signals disappear. The spectrum of the fully lithiated  $x = 0.5$  sample (**4**) shows only the presence of an intense “diamagnetic” cadmium site near +92 ppm as for the  $\text{Cd}^{\text{II}}[\text{Co}^{\text{III}}(\text{CN})_6]_{2/3}\cdot 4.7\text{H}_2\text{O}$  diamagnetic model compound,<sup>26</sup> indicating that all the Fe(III) ions are reduced. This result is fully consistent with earlier reports of a complete reduction of the Fe(III) sites in the hexacyanoferrate-based PBA electrode by lithiation.<sup>22,30</sup>

The spectra for the samples upon delithiation confirm the reversibility of the electrode reaction. The spectra of the  $x = 0.38$  and  $0.18$  samples upon delithiation (**5** and **6**) are similar to those of **3** and **2** respectively, with the following features: (i) the appearance of a significant amount  $\{\text{Cd}^{\text{II}}(\text{NC-Fe}^{\text{III}})_2(\text{dia})_4\}$  /  $\{\text{Cd}^{\text{II}}(\text{NC-Fe}^{\text{III}})_1(\text{dia})_5\}$  sites around -440 ppm for **5** and **6**; (ii) the presence of three cadmium sites for **6** with chemical shift values of -1000 ppm, -1325 ppm and -1520 ppm, that are ascribed to  $\{\text{Cd}^{\text{II}}(\text{NC-Fe}^{\text{III}})_3(\text{dia})_3\}$ ,  $\{\text{Cd}^{\text{II}}(\text{NC-Fe}^{\text{III}})_4(\text{dia})_2\}$  and  $\{\text{Cd}^{\text{II}}(\text{NCFe}^{\text{III}})_5(\text{dia})\}$  sites, respectively. Concerning the fully delithiated  $x = 0$  sample (**7**), except slight residual signals at low chemical shift, its spectrum is similar to that of the pristine one (**1**). Although a slight broadening of the Cd peaks due to a partial loss of crystallinity (*i.e.*, disorder at the local scale after (de)lithiation) is observed, overall NMR results show that the local electronic and structural features are recovered upon  $\text{Li}^+$  deintercalation, confirming the reversibility of the PBA electrode reaction.

In conclusion, we demonstrated that  $^{113}\text{Cd}$  NMR can be used as a sensitive local structural probe to monitor the lithium intercalation/deintercalation process inside a model PBA electrode based on  $\{\text{Cd-NC-Fe}\}$  units. The experimental observations are in agreement with the expected trends: (i) the Fe(III)/Fe(II) redox reaction is reversible; (ii) the maximum  $\text{Li}^+$  intercalation correspond to a full reduction of the Fe sites. However, new cadmium sites with lower chemical shifts are found upon lithiation. Importantly the NMR study shed light on the underlying electronic structure, in particular the possible occurrence of a fast charge transfer between Fe(III)/Fe(II) in the lithiated PBA. This feature might also be found in other FeM PBAs materials where the redox active sites are also the Fe ions. Further investigations on various PBA electrodes are now required to clarify this peculiar electronic state.

This work was financially supported by ANR-JST Strategic International Collaborative Research Program (SICORP),

Molecular Technology, Molecular Materials for Magnesium Batteries (MoMa).

## Notes and references

- a) J. Woodward, *Philos. Trans.* **1724**, 33, 15; b) F. Grandjean, F. Samarin, G.L. Long, *Dlaton Trans*, **2016**, *45*, 18018.
- a) S.S. Kaye, J. R. Long, *J. Am. Chem. Soc.*, **2005**, *127*, 6506; b) K.W. Chapman, P.D. Southon, C. L. Weeks, C.J. Kepert, *Chem. Commun.*, **2005**, 3322; c) L. Reguera, C. P. Krap, J. Balmaseda, E. Reguera, *J. Phys. Chem. C*, **2008**, *112*, 15893; d) P. K. Thallapally, R.K. Motkuri, C. A. Fernandez, B. P. McGrail, G. S. Behrooz, *Inorg. Chem.*, **2010**, *49*, 4909.
- P. Salazar, M. Martin, R.D. O’Neill, P. Lorenzo-Luis, R. Roche, J. L. Gonzales-Mora, in *Advanced Biomaterials and biodevices*, **2014**, Wiley, Ed. A. Tiwary, N. Nordin.
- a) A. Karyakin, E. Karyakina, L. Gorton, *Anal. Chem.*, **2000**, *72*, 1720-1723; b) A. S. Kumar, J. M. Zen, *Chem. Phys. Chem.* **2004**, *5*, 1227.
- a) O. Sato, T. Iyoda, A. Fujishima, K. Hashimoto, *Science*, **1996**, *271*, 704; b) S. Ferlay, T. Mallah, R. Ouahès, P. Veillet, M. Verdagner, *Nature*, **1995**, *378*, 701.
- M. Okubo, D. Asakura, Y. Mizuno, J. D. Kim, T. Mizokawa, T. Kudo, and I. Honma, *J. Phys. Chem. Lett.*, **2010**, *1*, 2063-2071.
- Y. Lu, L. Wang, J. Cheng, and J. B. Goodenough, *Chem. Commun.*, **2012**, *48*, 6544-6546.
- C. D. Wessells, S. V. Peddada, R. A. Huggins, and Y. Cui, *Nano Lett.*, **2011**, *11*, 5421-5425.
- C.D. Wessells, R.A. Huggins, Y. Cui, *Nat. Commun.*, **2011**, *2*, 550.
- Y. Mizuno, M. Okubo, E. Hosono, T. Kudo, K. Oh-ishi, A. Okazawa, N. Kojima, R. Kurono, S. Nishimura, and A. Yamada, *J. Mater. Chem. A*, **2013**, *1*, 13055-13059.
- A. L. Lipson, S. D. Han, S. Kim, B. F. Pan, N. Y. Sa, C. Liao, T. T. Fister, A. K. Burrell, J. T. Vaughey, and B. J. Ingram, *J. Power Sources*, **2016**, *325*, 646-652.
- Z. Li, K. Xiang, W. T. Xing, W. C. Carter, and Y. M. Chiang, *Adv. Energy Mater.*, **2015**, *5*, 1401410.
- M. Okubo, C. H. Li, and D. R. Talham, *Chem. Commun.*, **2014**, *50*, 1353-1355.
- D. Asakura, C. H. Li, Y. Mizuno, M. Okubo, H. S. Zhou, and D. R. Talham, *J. Am. Chem. Soc.*, **2013**, *135*, 2793-2799.
- C. H. Li, M. K. Peprah, D. Asakura, M. W. Meisel, M. Okubo, and D. R. Talham, *Chem. Mater.*, **2015**, *27*, 1524-1530.
- L. Wang, J. Song, R. Qiao, L. A. Wray, M. A. Hossain, Y. D. Chuang, W. Yang, Y. Lu, D. Evans, J. J. Lee, S. Vail, X. Zhao, M. Nishijima, S. Kakimoto, and J. B. Goodenough, *J. Am. Chem. Soc.*, **2015**, *137*, 2548-2554.
- A. Ulvestad, A. Singer, J. N. Clark, H. M. Cho, J. W. Kim, R. Harder, J. Maser, Y. S. Meng, and O. G. Shpyrko, *Science*, **2015**, *348*, 1344-1347.
- J. Lim, Y. Li, D. H. Alsem, H. So, S. C. Lee, P. Bai, D. A. Cogswell, X. Liu, N. Jin, Y. S. Yu, N. J. Salmon, D. A. Shapiro, M. Z. Bazant, T. Tyliczszak, and W. C. Chueh, *Science*, **2016**, *353*, 566-571.
- E. McCalla, A. M. Abakumov, M. Saubanere, D. Foix, E. J. Berg, G. Rousse, M. L. Doublet, D. Gonbeau, P. Novak, G. Van Tendeloo, R. Dominko, and J. M. Tarascon, *Science*, **2015**, *350*, 1516-1521.
- B. Mortemard de Boisse, G. Liu, J. Ma, S. Nishimura, S. C. Chung, H. Kiuchi, Y. Harada, J. Kikkawa, Y. Kobayashi, M. Okubo, and A. Yamada, *Nat. Commun.*, **2016**, *7*, 11397.
- Y. Nanba, T. Iwao, B. Mortemard de Boisse, W. Zhao, E. Hosono, D. Asakura, H. Niwa, H. Kiuchi, J. Miyawaki, Y. Harada, M. Okubo, and A. Yamada, *Chem. Mater.*, **2016**, *28*, 1058-1065.

- 22 a) Y. Mizuno, M. Okubo, K. Kagesawa, D. Asakura, T. Kudo, H. S. Zhou, K. Oh-ishi, A. Okazawa, N. Kojima, *Inorg. Chem.* (2012) 51, 10311; b) M. Okubo, D. Asakura, Y. Mizuno, T. Kudo, H. Zhou, A. Okazawa, N. Kojima, K. Ikedo, T. Mizokawa, I. Honma, *Angew. Chem. Int. Ed.* (2011) 50, 6269;
- 23 M. Wagemaker, A. P. M. Kentgens, and F. M. Mulder, *Nature*, 2002, 418, 397-399.
- 24 R. Bhattacharyya, B. Key, H. L. Chen, A. S. Best, A. F. Hollenkamp, and C. P. Grey, *Nat. Mater.*, **2010**, 9, 504-510.
- 25 Y. Y. Hu, Z. G. Liu, K. W. Nam, O. J. Borkiewicz, J. Cheng, X. Hua, M. T. Dunstan, X. Q. Yu, K. M. Wiaderek, L. S. Du, K. W. Chapman, P. J. Chupas, X. Q. Yang, and C. P. Grey, *Nat. Mater.*, **2013**, 12, 1130-1136.
- 26 A. Flambard, F. H. Kohler, and R. Lescouëzec, *Angew. Chem. Int. Ed.*, **2009**, 48, 1673-1676.
- 27 A. Flambard, F. H. Kohler, R. Lescouëzec, and B. Revel, *Chem. Eur. J.*, **2011**, 17, 11567-11575.
- 28 J.D. Cafun, G. Champion, M.-A. Arrio, C. Cartier dit Moulin, A. Bleuzen, *J. Am. Chem. Soc.* **2010**, 132, 11552-11559.
- 29 W. Weppner, R. A. Huggins, *J. Electrochem. Soc.*, **124**, **1977**, 124, 1569
- 30 D. Asakura, M. Okubo, Y. Mizuno, T. Kudo, H. S. Zhou, K. Amemiya, F. M. F. de Groot, J. L. Chen, W. C. Wang, P. A. Glans, C. L. Chang, J. H. Guo, and I. Honma, *Phys. Rev. B*, **2011**, 84, 045117.
- 31 a) T. L. Greaves, J.D. Cashion, *Hyperfine Interact.* 237, **2016**, 70; b) A. I. Rykov, J. Wang, T. Zhang, K. Nomura, *Hyperfine Interact.* 218, **2013**, 53.